ORNL/SR-2016/503

Evaluation of Lower East Fork Poplar Creek Mercury Sources—Model Update

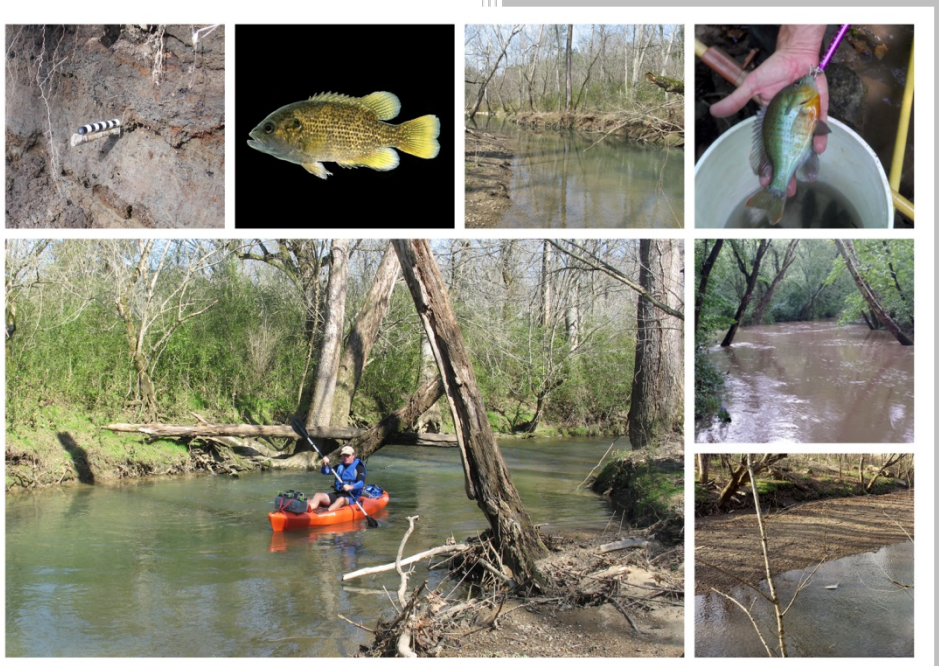

David Watson
Mark Bevelhimer
Craig Brandt
Chris DeRolph
Scott Brooks
Melanie Mayes
Todd Olsen
Johnbull Dickson
Mark Peterson
Richard Ketelle

September 2016

OAK RIDGE NATIONAL LABORATORY
MANAGED BY UT-BATTELLE FOR THE US DEPARTMENT OF ENERGY

ORNL/SR-2016/503

Environmental Sciences Division

EVALUATION OF LOWER EAST FORK POPLAR CREEK MERCURY SOURCES—MODEL UPDATE

David Watson
Mark Bevelhimer
Craig Brandt
Chris DeRolph
Scott Brooks
Melanie Mayes
Todd Olsen
Johnbull Dickson
Mark Peterson
Richard Ketelle

Date Published: September 2016

Prepared for
Lynn Sims, UCOR/RSI
Oak Ridge, TN 37831-7293

Prepared by
OAK RIDGE NATIONAL LABORATORY
Oak Ridge, TN 37831-6283
managed by
UT-BATTELLE, LLC
for the
US DEPARTMENT OF ENERGY
under contract DE-AC05-00OR22725

CONTENTS

LIST OF FIGURES

LIST OF TABLES

ACRONYMS

BER	bank erosion rate
cms	cubic meters per second
DOE	US Department of Energy
EFK	East Fork Poplar Creek kilometer
EFPC	East Fork Poplar Creek
EM	Environmental Management
FY	fiscal year
FYR	Five Year Review
Hg	mercury
HgT	total mercury
HRD	historical release deposit
IHg	inorganic mercury
LEFPC	lower East Fork Poplar Creek
MeHg	methylmercury
MeHgT	total methylmercury
OF200	Outfall 200
ORNL	Oak Ridge National Laboratory
ORWTF	Oak Ridge Wastewater Treatment Facility
SFA	Science Focus Area
TD	Technology Development
TSS	total suspended solids
UEFPC	upper East Fork Poplar Creek
WEMA	West End Mercury Area
Y-12	Y-12 National Security Complex

1. INTRODUCTION

The purpose of this report is to assess new data that has become available and provide an update to the evaluations and modeling presented in the Oak Ridge National Laboratory (ORNL) Technical Manuscript Evaluation of lower East Fork Poplar Creek (LEFPC) Mercury Sources (Watson et al., 2016). Primary sources of field and laboratory data for this update include multiple US Department of Energy (DOE) programs including Environmental Management (EM; e.g., Biological Monitoring and Abatement Program, Mercury Remediation Technology Development [TD], and Applied Field Research Initiative), Office of Science (Mercury Science Focus Areas [SFA] project), and the Y-12 National Security Complex (Y-12) Compliance Department.

The Watson et al. (2016) report summarizes the 3-year research project undertaken to better understand the nature and magnitude of mercury (Hg) fluxes in LEFPC. The project/report addresses the requirements of Action Plan 1 in the 2011 Oak Ridge Reservation-wide Comprehensive Environmental Response, Compensation, and Liability Act Five Year Review (FYR). The Action Plan is designed to address a twofold 2011 FYR issue: (1) new information suggests mobilization of mercury from the upper and lower EFPC streambeds and stream banks is the primary source of mercury export during high-flow conditions, and (2) the current Record of Decision did not address the entire hydrologic system and creek bank or creek bed sediments.

To obtain a more robust watershed-scale understanding of mercury sources and processes in LEFPC, new and existing data from multiple DOE programs were compiled and assessed to develop a conceptual model (see Fig. 1) and a dynamic numerical watershed and bioaccumulation model (see Fig. 2). The goal of the assessments and modeling was to generate a more holistic and quantitative understanding of the watershed and the sources, flux, concentration, transformation, and bioaccumulation of inorganic mercury (IHg) and methylmercury (MeHg).

Model development used a hybrid approach that dynamically linked a spreadsheet-based physical and chemical watershed model to a systems dynamics, mercury bioaccumulation model for key fish species. The watershed model tracks total Hg (HgT) and MeHg fluxes and concentrations by examining upstream inputs, floodplain runoff, floodplain leaching, bank soil erosion, and periphyton matrix dynamics (Fig. 2). The bioaccumulation model tracks the feeding, growth, and mercury assimilation of representative individual fish through their typical life span using key inputs of fish size, water temperature, and diet. The LEFPC watershed was divided into five modeling reaches, and fluxes and concentrations are assessed at this spatial scale (see Fig. 3). The following are the key findings of the field and laboratory studies and the watershed and bioaccumulation modeling (Watson et al., 2016):

- The greatest flux of HgT in LEFPC is related to stormflow transport of Hg-contaminated solids entering the creek because of bank erosion in the upper reaches of the creek.
- The second greatest flux originates from upper EFPC (UEFPC) and appears to control base flow fluxes (Station 17 representing the exit stream sampling point near the boundary of the Y-12 Complex).
- The observed increase in MeHg concentration and flux from upstream to downstream is related primarily to instream methylation by periphyton and other biological activity.
- A meaningful substantial reduction of the HgT flux in LEFPC would require addressing the flux of HgT originating from bank erosion and from Station 17.
- Actions to reduce LEFPC floodplain leaching and runoff would not produce much of an impact on HgT or MeHg concentrations or fluxes unless other major sources are eliminated first.

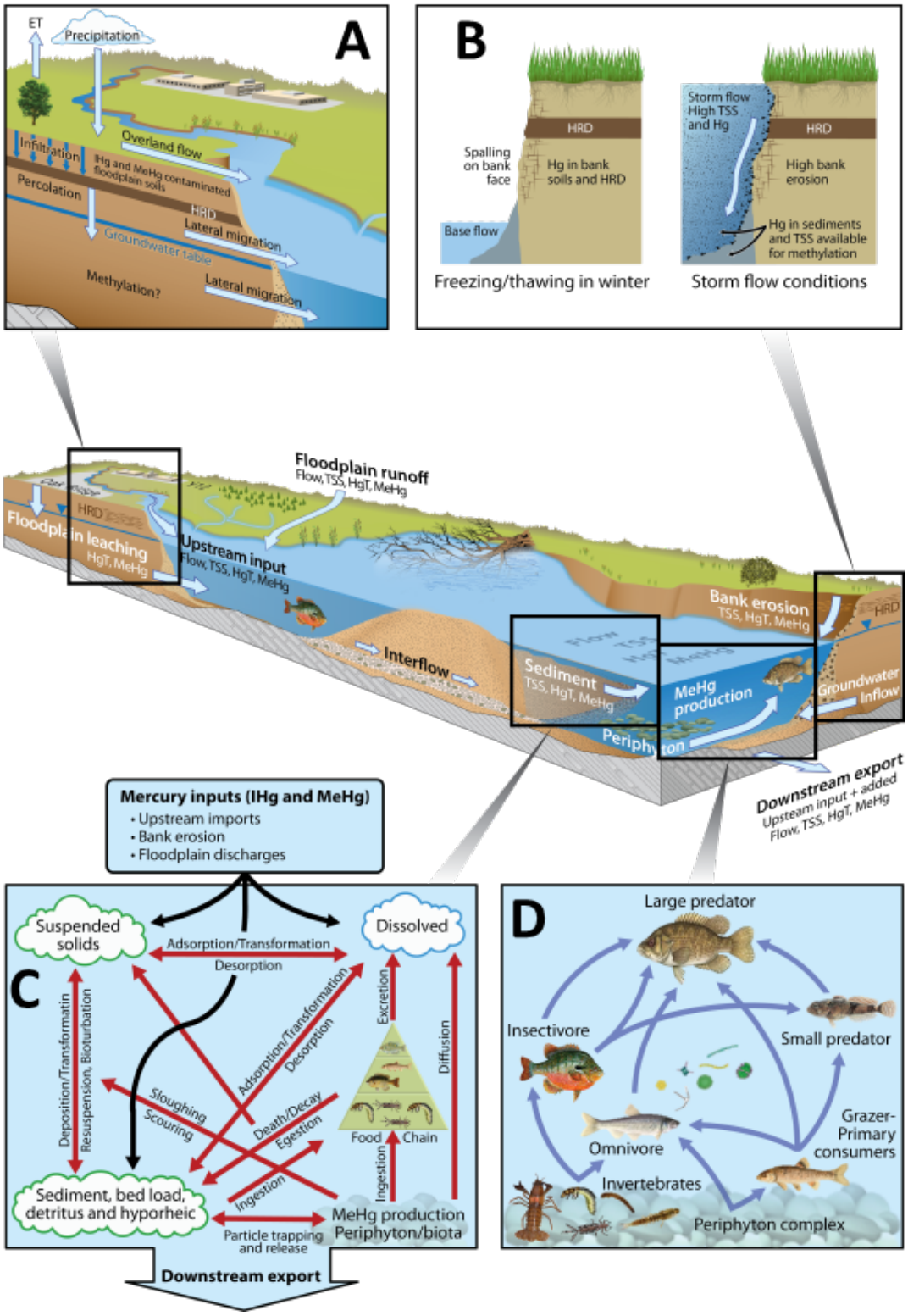

Fig. 1. Conceptual model for understanding mercury source contributions to Lower East Fork Poplar Creek from floodplain (A) and bank soil (B) and instream mercury processes (C) including bioaccumulation (D). (*Notes:* TSS = total suspended solid; HgT = total mercury; MeHg = methylmercury; HRD = Historical release deposits.)

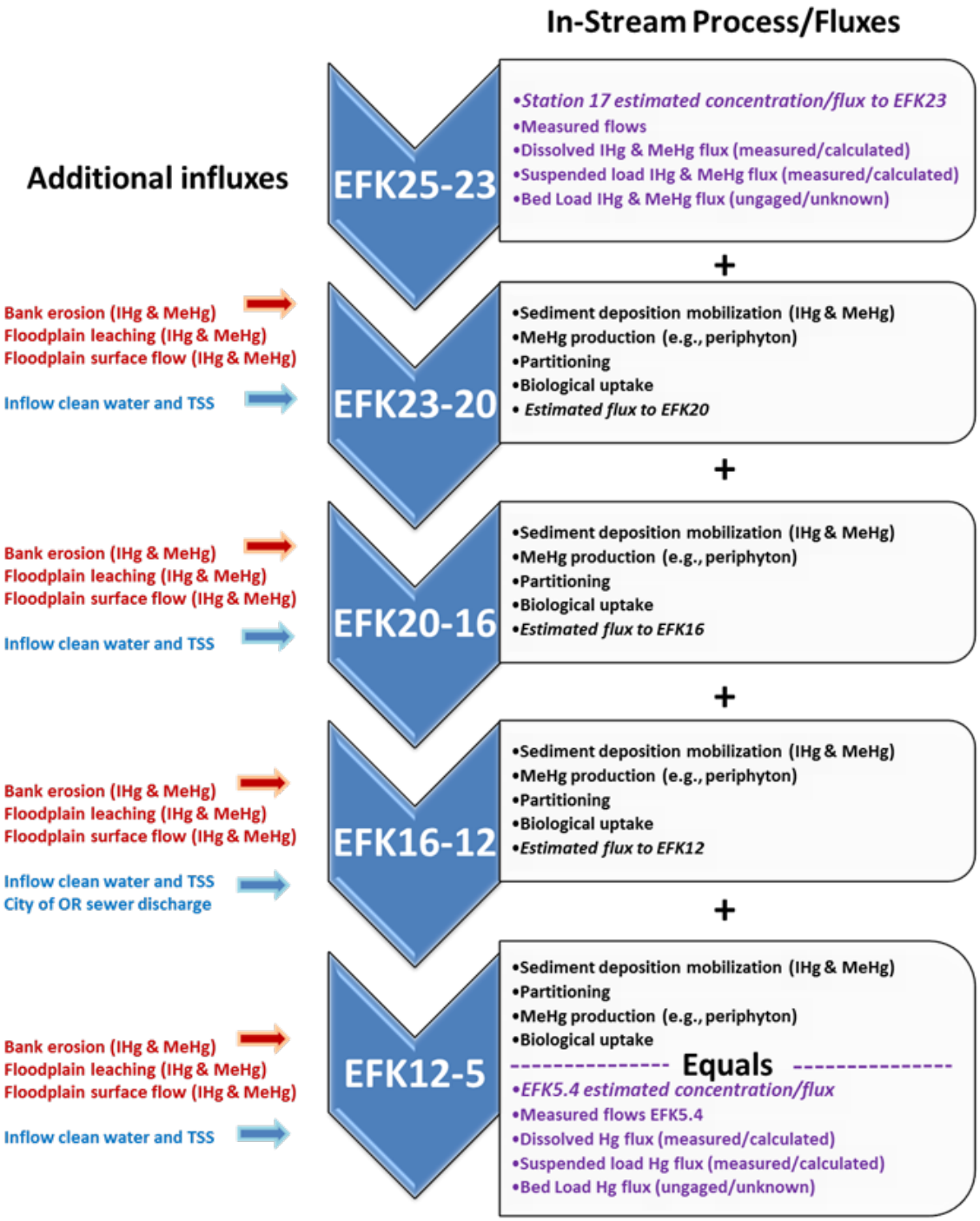

Fig. 2. Model framework showing stream reaches, inorganic mercury (IHg), and methylmercury (MeHg) inflow and outflow, and instream processes considered in the model.
(*Notes:* EFK = East Fork Poplar Creek kilometer; TSS = total suspended solids.)

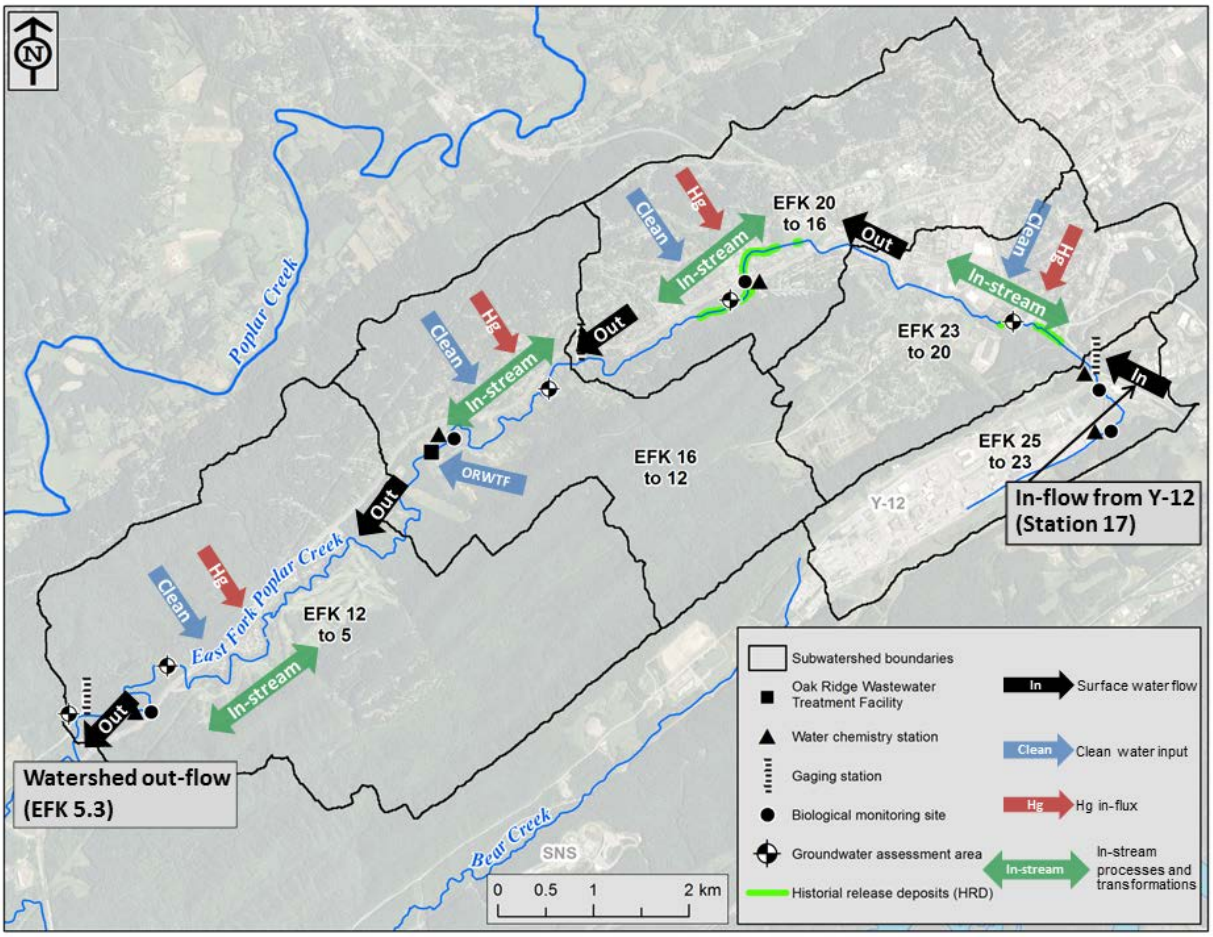

Fig. 3. Subwatershed boundaries and key fluxes and inputs. (*Notes:* EFK = East Fork Poplar Creek kilometer; Hg = mercury; ORWTF = Oak Ridge Wastewater Treatment Facility; SNS = Spallation Neutron Source; Y-12 = Y-12 National Security Complex.)

This project addresses the Action Plan goal to evaluate the role of LEFPC bank soil sources and to consider the entire EFPC hydrologic system. Since a robust understanding and quantification of some mercury-related parameters and relationships is still lacking, the conceptual model and numerical model configuration and predictions are dependent on the data available at the time of the assessment. Therefore, there is a need for continued data collection and model improvements. Model predictions should be viewed cautiously, with comparisons of the magnitude of predictions between scenarios being more valid than predictions of absolute concentrations or fluxes. With continued updates and refinement, the watershed-scale model can be a useful, valuable tool for future EFPC research prioritization, technology development, and remedial decision-making.

For this report, new data not included in Watson et al. (2016) but relevant to determining model inputs was assessed to determine if changes in the conceptual and numerical models presented in Watson et al. (2016) are warranted (Section 2). Where appropriate, the new data/inputs were entered into the models, which were rerun to determine the magnitude of changes in the predictions of IHg and/or MeHg concentrations and fluxes (Section 3). The inclusion of new data into the watershed model produces output in terms of the amount of MeHg produced in the creek that can then be incorporated as new input into the fish bioaccumulation model. In addition to updated model input in terms of MeHg concentrations in the periphyton matrix, several improvements to the bioaccumulation model were made this year in a continued effort to enhance and refine the model processes and mechanisms.

2. ASSESSMENT OF NEW DATA AND MODEL INPUT PARAMETERS

The data and model inputs can be divided into the following general categories:

- Flow and mercury flux estimates at Station 17 (Inflow) and East Fork Poplar Creek kilometer (EFK) 5.4 (Outflow)
- Bank erosion estimates
- Floodplain inputs—Overland flow and infiltration
- Instream IHg and MeHg processes
- Estimates of mercury concentration on total suspended solids (TSS)
- Estimates of HgT and MeHg in periphyton
- Estimates of mercury concentrations in fish tissue (described in Section 3.2)

For each of these categories, a discussion is provided below on whether new data (1) was identified, (2) provides any insights into mercury cycling processes, (3) changes any assumptions previously made regarding IHg or MeHg concentrations and/or fluxes, and (4) could significantly change model inputs and predictions of mercury concentrations or fluxes. This report focuses heavily on incorporating and assessing new bank erosion data. That effort is warranted because bank erosion is thought to be one of the largest sources of mercury entering LEFPC and, although there is still considerable uncertainty, the new data made it possible to refine the bank erosion estimates.

2.1 FLOW AND MERCURY FLUX ESTIMATES AT STATION 17 (INFLOW) AND EFK 5.4 (OUTFLOW)

The model was set up to represent typical average monthly flow conditions with flow augmentation in UEFPC turned off because that is the current and likely future condition. Flow augmentation (~0.2 cubic meters/second [cms]) was discontinued in May 2014, so when the model was being developed there was only limited flow and mercury concentration data available representative of conditions with flow augmentation shut off. For the original model, it was estimated that, based on past data, monthly average flows at Station 17 (without flow augmentation) would vary between 0.24 cms in January and February and 0.17 cms in August and October. Since flow augmentation was shut off in May 2014, the average flow at Station 17 over a ~2 year period was estimated from Station 17 flow gaging data to be approximately 0.18 cms. Although 0.18 cms may be slightly lower than the average used in the model, the difference is probably not significant enough to impact watershed scale flow predictions and may just be related to natural variation in flows that would be expected from year to year.

As reported in Leidos (2016), since 2011 the HgT flux at Station 17 has decreased each year, including through FY 2015 (Leidos, 2016). The HgT flux at Station 17 was estimated to be 8.1 kg/yr in 2015. In 2014, it was estimated to be 14.4 kg/yr, but the higher flux in 2014 is likely a remnant of the elevated mercury discharge that started in fiscal year (FY) 2011 due to the West End Mercury Area (WEMA) storm drain cleanout actions.

The HgT flux for Station 17 used in the model was 9.8 kg/yr, which is somewhat higher than the 8.1 kg/yr flux reported in Leidos (2016) for 2015. It is not known if the reduction in HgT flux at Station 17 will continue or will start to fluctuate from year to year. To test the watershed level impact of the somewhat lower HgT flux measured at Station 17 in 2015, the Station 17 flux was reduced to 8.1 kg/yr in the model; as expected, there was a resultant decrease in the watershed HgT flux of 1.7 kg/yr. However, the

predicted concentration of MeHg in periphyton in LEFPC, which is thought to control the MeHg uptake in fish, did not change very much, if at all, with the reduction of HgT used in the model for Station 17. It should be noted that the annual flux of MeHg at Station 17 is not currently measured, but it did not make much difference in the prediction of periphyton MeHg concentrations if the MeHg flux at Station 17 was assumed to stay the same or was reduced by an amount comparable to the HgT flux. Flow weighted mercury (IHg or MeHg) sampling is not being conducted at EFK 5.4, so no new annual flux measurements are available for that location.

Based on these evaluations and new flow and mercury flux measurements that are available, permanent changes to the model do not appear to be warranted. However, it is recommended that the HgT and MeHg fluxes at Station 17 and EFK 5.4 be monitored and the model updated as the fluxes are reduced more substantially due to remedial actions such as the construction of the Outfall 200 (OF200) treatment plant, Y-12 facility operation modifications, or continued recovery from the WEMA outfall actions.

2.2 BANK EROSION ESTIMATES

Bank erosion is believed to be a key source of IHg and, to a lesser extent, MeHg to LEFPC, particularly during high flow storm events when erosion rates are high. As described in Watson et.al. (2016), to estimate the flux of IHg and MeHg to UEFPC, Geographical Information System analysis tools were used to associate bank erosion rates (BERs) determined by the kayak analysis with the closest longitudinal bank sampling location and the concentrations of IHg and MeHg detected at that location. Where historical release deposits (HRDs) with high concentrations of HgT were known to exist, a single average whole bank profile concentration for the HRD (157 mg/kg for HgT) was associated with the BER and used to determine the flux of HgT and MeHg. These estimates of HgT and MeHg fluxes were then summed to determine estimates for each 100 m incremental stream segment for plotting purposes, and then summed to obtain bank HgT and MeHg flux estimates for each modeling reach. The calculated average concentration of HgT and MeHg in bank soils for each reach was also calculated. From this analysis, the total HgT and MeHg fluxes resulting from bank erosion for all the LEFPC reaches were estimated to be 38.6 kg/year and 5.6 g/year, respectively. For estimating monthly inputs to the model, it was assumed that there would be, on average for most years, greater erosion rates during wetter high-flow months (winter and spring) and also greater erosion during periods of alternating freezing and thawing (winter, and to a lesser extent, late fall and early spring) that would result in soil spalling. For purposes of maintaining a mass balance in the model, the total HgT bank erosion flux was assumed to be 0.7 times (i.e., ~26 kg/year) the total estimate as calculated above (i.e., 38.6 kg/year). In the original version of the model, the calibration factor (0.7) was not applied to estimates of MeHg bank erosion flux.

Since the model was first developed (Watson et al., 2016), additional characterization of the HRD has been completed as part of the Mercury TD project, including the following:

- Field mapping of the visual extent of the HRD (see Fig. 4)
- Sampling of the HRD and HgT analysis (~35 locations with up to three depths at each location) and MeHg analysis (~21 locations at one depth)
- Vertical bank sampling from top to bottom at four new locations (~64 samples) and analysis of HgT concentrations

This new bank characterization data, which will be described in greater detail in the FY 2016 Mercury TD annual project report (Peterson et al. 2016), has substantially improved the current understanding of the lateral extent and concentration of the HRD and the vertical profile of HgT in the stream bank where the HRD has been observed. The average HgT concentration for the HRD is approximately 695 mg/kg, but the vertical average concentration for the whole bank is significantly lower (~195 mg/kg for six vertical

profiles), with the vertical average considered more relevant and appropriate for estimating mercury fluxes from bank erosion where the HRD is present.

Fig. 4. Extent of the historical release deposit (HRD) based on field mapping.
(*Notes:* LEFPC = Lower East Fork Poplar Creek; Y-12 = Y-12 National Security Complex.)

Figure 5 shows that there is excellent correlation ($r^2 = 0.97$) between the maximum detected HRD concentration and the average HgT concentration measured for six vertical bank profiles conducted at a different locations. To provide a better estimate of the spatial distribution of HgT bank erosion flux where the HRD is present, this relationship (HgT bank avg. = 0.1393 × HgT HRD max.) was used to estimate the vertical average bank concentration at the ~35 locations where the HRD was sampled (see Fig. 6). These new spatially variable estimates of the vertical bank average concentrations where the HRD is present were than associated as before with the BERs estimated from the kayak study. The average MeHg concentration detected from the recent HRD bank sampling, 23.4 µg/kg, was used in place of previous estimates of the MeHg concentrations for bank soils containing HRD. Comparisons of the revised and original bank erosion flux estimates for HgT and MeHg are shown in Figs. 7 and 8, respectively. These figures show several areas in the upper reaches of LEFPC where the revised estimates of HgT and MeHg bank erosion fluxes, respectively, increased. Although Figs. 7 and 8 provide an indication of the location and potential relative magnitude of where bank erosion fluxes may be elevated, it should be noted that there is considerable uncertainty in these estimates, and to maintain mass balance, the bank erosion calibration factor had to be modified from 0.7 to 0.43. This revised calibration factor (i.e., 0.43) was also applied to the MeHg bank fluxes, which had the impact of reducing the estimated fluxes of MeHg from bank erosion compared with the original model. The impacts of these revised estimates of bank erosion fluxes on the model results are discussed further in Section 3.

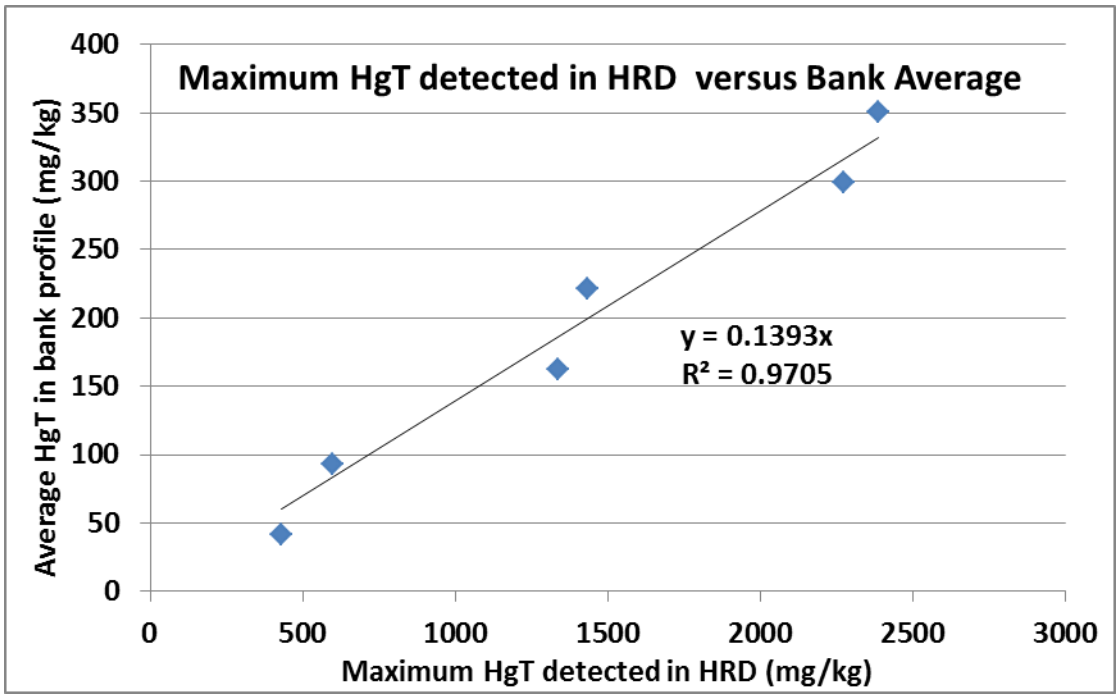

Fig. 5. Relationship between historical release deposit (HRD) maximum concentration and the average HgT concentration for the whole bank profile.

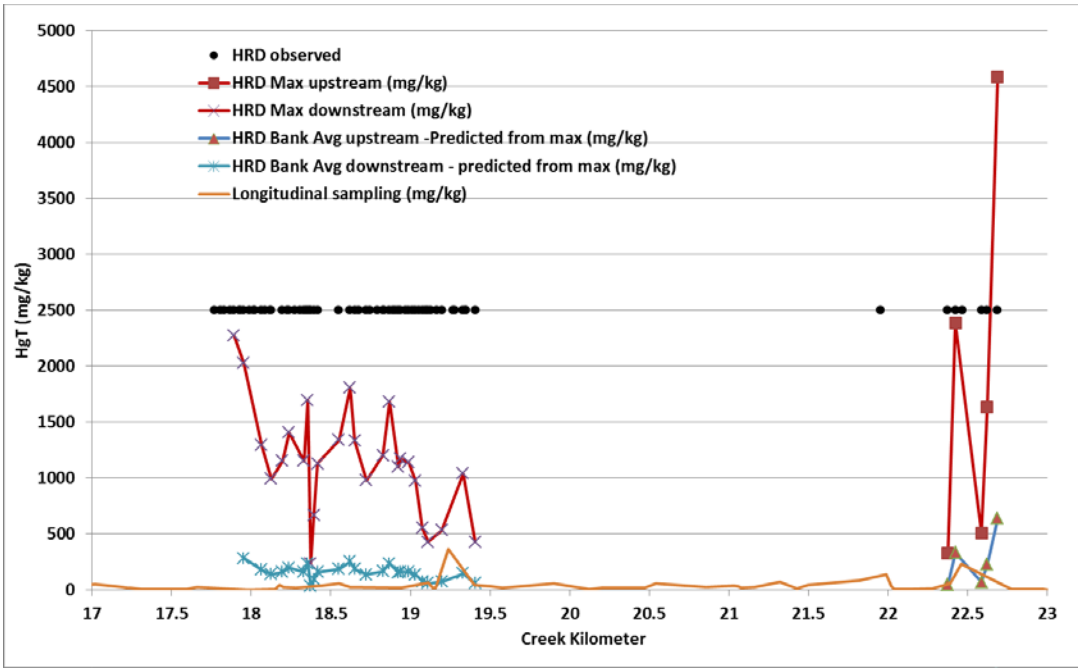

Fig. 6. Comparison of estimated vertical average HgT bank concentration in lower East Fork Poplar Creek (based on historical release deposit [HRD] HgT maximum and vertical bank profile average shown in Fig. 5) to maximum HRD concentration detected at each HRD sampling location and longitudinal bank sampling data. Location of HRD is shown with dots.

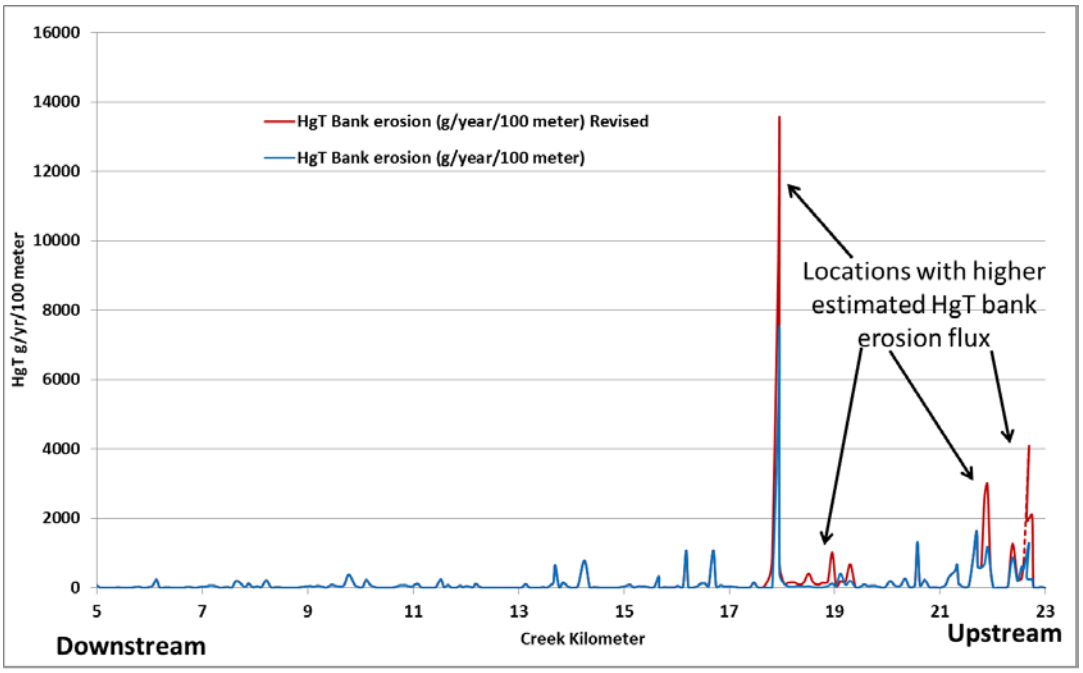

Fig. 7. Comparison of revised and original bank erosion HgT flux estimates per 100 m reach showing areas with increased flux.

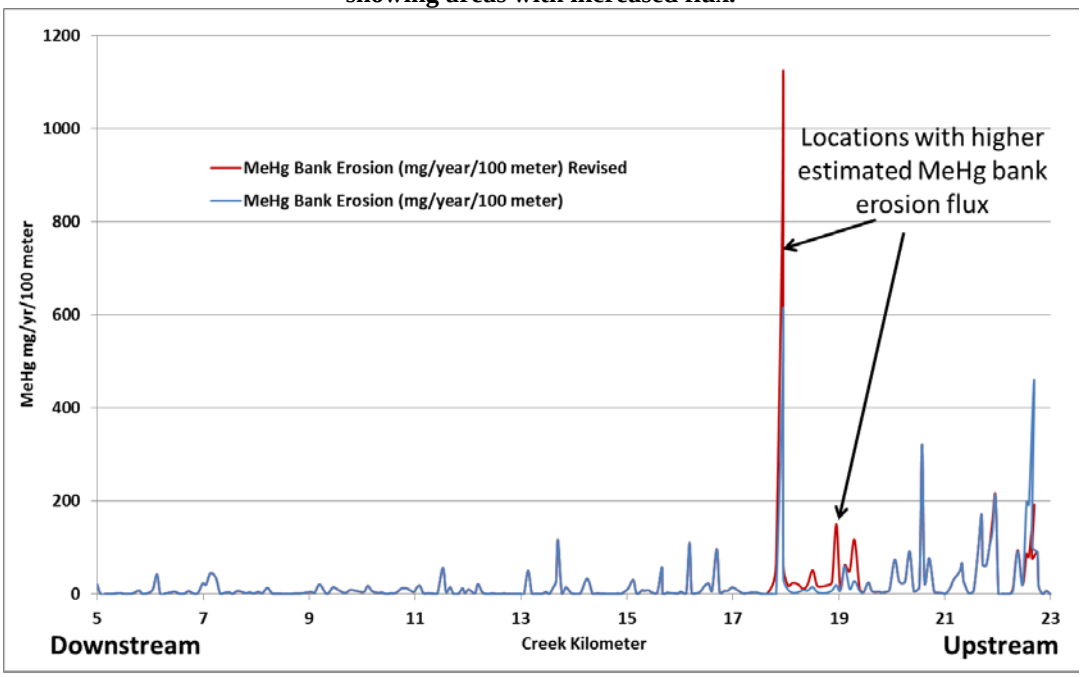

Fig. 8. Comparison of revised and original bank erosion MeHg flux estimates per 100 m reach showing areas with increased flux.

2.3 FLOODPLAIN INPUTS—OVERLAND FLOW AND INFILTRATION

As part of the Mercury TD project, three new well clusters (three wells each) were installed in the LEFPC floodplain, and the groundwater was sampled five different times and analyzed for HgT and MeHg. This new groundwater characterization data will be described in greater detail in the FY 2016 Mercury TD

project annual report (Peterson et al. 2016). The average MeHg concentration detected for all the wells was 4.1 ng/L with a maximum MeHg concentration of 27.4 ng/L. The average HgT was 10.6 ng/L for all wells with a maximum HgT concentration of 71 ng/L. Methodology used to estimate the MeHg fluxes due to leaching of mercury-contaminated floodplain sediments for the model is described in Watson et al. (2016). The average HgT concentration in the model was estimated to be 53.3 ng/L, and the MeHg concentration from leaching was calculated to be 8.0 ng/L, assuming the MeHg concentration is 0.15 of the estimated HgT floodplain leaching based on the limited previous well sampling data that was available at the time (Watson et al., 2016). The new HgT and MeHg well data concentrations are lower but similar to the model estimates and judged to be within the bounds of what spatial and sampling variability could be. The original estimated HgT and MeHg floodplain leaching fluxes were low relative to other sources of mercury fluxes in the LEFPC watershed; incorporating this new data into the model would likely make the estimates even lower but not have a significant impact on any of the conclusions presented in Watson et al. (2016).

No additional data was collected that would impact estimates of the overland flow fluxes of mercury from the floodplain.

2.4 INSTREAM MERCURY PROCESSES

Sediment sampling and mercury analysis have recently been conducted as part of the Mercury TD project and will be described in greater detail in the FY 2016 Mercury TD project annual report (Peterson et al. 2016). Figure 9 shows HgT concentrations in fine, medium, coarse, and bulk LEFPC sediment fraction compared with longitudinal bank sampling data and the location of the HRD. The concentration trends are spatially complex, but in general, upstream of EFK 23, onsite Y-12 sources of sediment have fine fractions with the highest HgT concentrations of all the fractions, and the coarse fraction has the lowest concentration. Downstream of EFK 23, erosion of the banks and HRD seem to provide HgT source material that have higher concentrations of mercury in the medium to coarse fractions, and the concentration of mercury in the fines seems to be reduced by the influx of uncontaminated fines from the rest of the watershed. Increases in LEFPC sediment concentrations around EFK 11 may suggest another bank source in this area and/or deposition of sediments from upstream. Bulk HgT concentrations track closely with the medium sediment fraction (especially downstream), probably because the medium fraction makes up the greatest weight percentage of the sediment fractions.

Figure 10 shows the MeHg concentrations in fine, medium, coarse, and bulk LEFPC sediment fraction compared with longitudinal bank sampling data and the location of the HRD. The spatial trends are complex, but in general, the MeHg in sediment decreases from upstream to downstream, with the exception that the coarse and bulk fractions are significantly elevated between EFK 19 and EFK 24, especially compared with the other sediment fractions. It is possible that the elevated MeHg in the coarse sediment fraction in this reach between EFK 19 and EFK 24 is partially related to bank erosion. In general, the MeHg concentrations in the sediments are lower than the concentrations that have been detected in periphyton and have an opposite concentration trend, where MeHg is generally higher in periphyton further downstream. These data seem to confirm that the increasing MeHg concentration trends downstream in LEFPC surface water are primarily related to periphyton (Olsen et al., 2016) and other biological production mechanisms rather than from sediment-related sources.

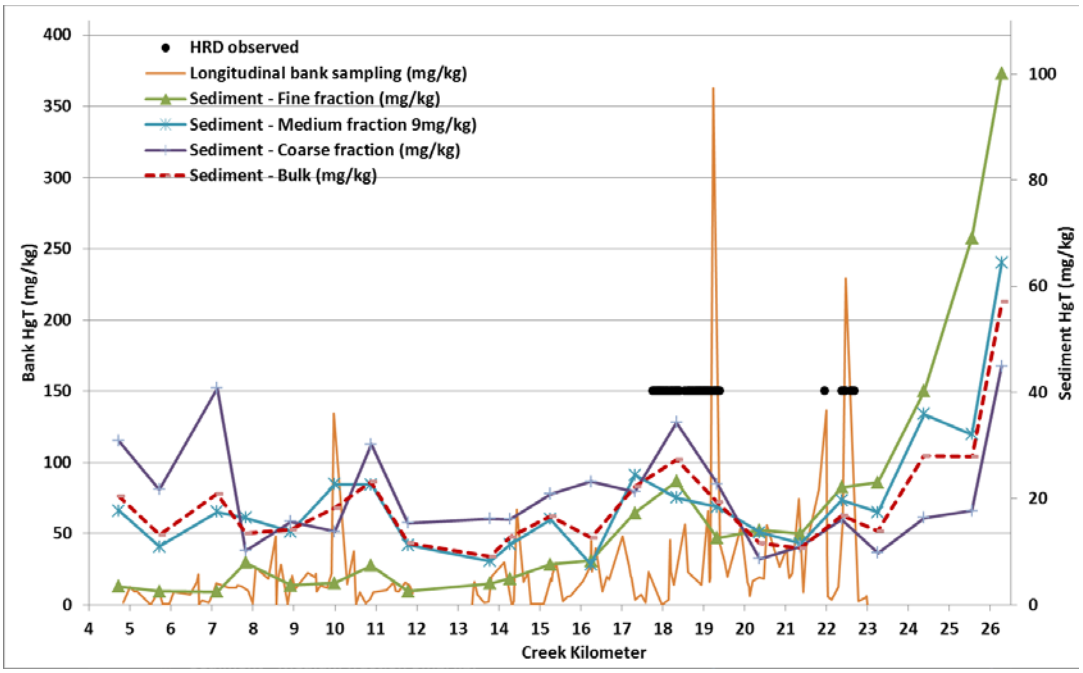

Fig. 9. HgT concentration in fine, medium, coarse, and bulk sediment fraction compared with longitudinal bank sampling data; location of HRD is shown with dots.

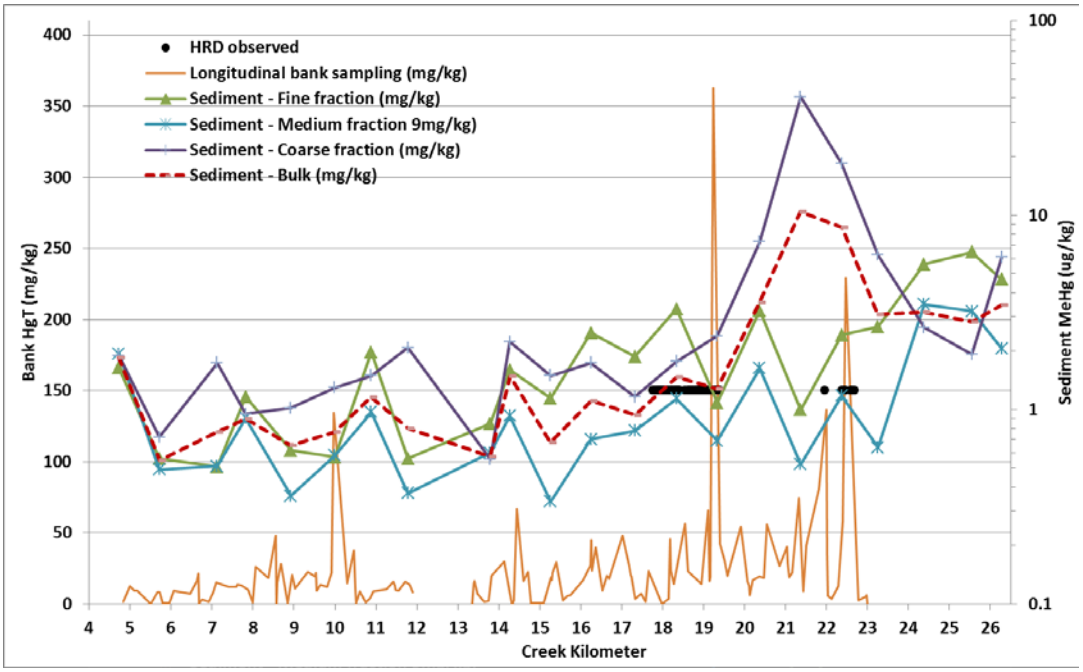

Fig. 10. MeHg concentration in fine, medium, coarse, and bulk sediment fraction compared with longitudinal bank sampling data; location of HRD is shown with dots.

The new sediment data could inform a more mechanistic sediment and bedload transport module if, as recommended in Watson et al. (2016), these processes are incorporated into the model when LiDAR elevation data become available in FY 2017. In addition, if mechanistic understanding of the causes of the

spatial variability that are observed in the different size fractions of the sediment and other data is developed through the mercury TD or SFA projects, further discretization of the model into 1.0 km or smaller subwatershed segments is recommended to improve predictive capabilities of the model.

Besides the sediment data, there was not sufficient new water quality monitoring data available to impact the current assumptions used to simulate the instream HgT and MeHg processes (e.g., methylation rates). However, since the EFPC is a dynamic, rapidly changing system because of Y-12 Complex modifications and other factors, it is recommended that as additional data is collected in the next FY, the assumptions used in the model for instream processes be reassessed and validated.

2.5 MERCURY CONCENTRATION ON TOTAL SUSPENDED SOLIDS (TSS)

The concentration of HgT associated with TSS is used in the model as an indicator of the concentration of IHg that would be available to periphyton for methylation. The concentration of HgT on TSS at any point along the creek is impacted by the TSS concentration entering at Station 17, the concentration of HgT on bank sediments entering the creek, the concentration of TSS in floodplain runoff (~17 mg/kg), and the amount of clean TSS that enters the system because of runoff from uncontaminated portions of the LEFPC watershed. Because assumptions regarding bank erosion fluxes were revised due to the new HRD characterization data, the TSS assessment also needed to be revised. Table 1 shows a comparison of the original model inputs for the HgT and MeHg average bank concentrations for each modeling reach and the revised assumptions that incorporate new data on the HRD extent and concentrations. Incorporating the new HRD characterization data resulted in significantly higher estimates of HgT concentrations in the two upper reaches of LEFPC but had no impact on the two lower reaches. For MeHg the average bank concentration increased in the second reach, was lower in the first reach, and remained the same in the two lower reaches (Table 1). The revised HgT bank concentrations were than used to estimate revised average HgT concentrations on TSS for each of the LEFPC subwatersheds (see Table 2). To maintain mass balance, the estimated fluxes of HgT bank erosion were multiplied by a calibration reduction factor of 0.43. The revised TSS HgT concentrations are slightly higher in the upper two reaches of LEFPC than what it was in the original model, but the same HgT TSS concentration of 80 mg/kg was used as input to the first reach representing the input from Station 17. These revised results appear to be reasonable for use as model inputs in the revised model.

Table 1. Original compared with revised total mercury (HgT) and methylmercury (MeHg) bank concentrations per modeling reach incorporating new understanding of the HRD

Stream reach	Original model		Revised model	
	HgT concentration (mg/kg)	MeHgT concentration (µg/kg)	HgT concentration (mg/kg)	MeHgT concentration (µg/kg)
EFK 23 to 20	60	12.2	133	10.2
EFK 20 to 16	80	7.4	144	13.8
EFK 16 to 12	8.7	1.3	8.7	1.3
EFK 12 to 5	11.9	1.9	11.9	1.9

Table 2. Comparison of revised estimates of total mercury (HgT) on total suspended solids (TSS) with original model estimates and estimates from past mercury Science Focus Area sampling

Location	TSS concentration revised (mg/kg)	TSS concentration original (mg/kg)	TSS concentration measured (mg/kg)
EFK 23 to 20	48	46	55

EFK 20 to 16	39	36	36
EFK 16 to 12	25	25	25
EFK 12 to 5	17	17	17
Station 17 input	80	80	NA

2.6 MERCURY IN PERIPHYTON

As described in Watson et al. (2016), there is a high degree of variability in the periphyton data. However, similar to what is observed in aqueous samples, the concentrations of MeHg generally increase in the downstream direction, whereas HgT decreases. It was assumed for the model that MeHg concentrations near Station 17 are typically in the 5 ng/g range, whereas farther downstream they can be >20 ng/g when biological activity is high in the warmer months. In the model, a calibration factor was applied to the predicted MeHg aqueous concentration to estimate the MeHg concentration in periphyton on a monthly basis. Based on the available data, HgT concentrations in periphyton were assumed to range from ~20 mg/kg in model reach EFK 23–20 to ~4.5 mg/kg near EFK 5.4. For the model, the concentration of HgT in periphyton was assumed to be related to the estimated HgT concentration on TSS and to be relatively constant on a monthly basis (i.e., not change seasonally). A calibration factor was applied to the TSS HgT concentration data to estimate the HgT concentration in periphyton for each stream reach. These concepts are shown in Fig. 11.

The Mercury SFA project has continued to conduct sampling and analysis activities to characterize the concentration of mercury in LEFPC periphyton. There is considerable variability in the MeHg concentrations determined for periphyton both spatially and over time, with MeHg concentrations in LEFPC ranging from <1.0 ng/g to 57 ng/g dry weight. The variability in MeHg concentrations appears to indicate that there are complex localized environmental and biological factors controlling MeHg production in LEFPC. Despite this variability, there seems to be a general trend of higher MeHg in periphyton in middle to lower stream reaches than in upper reaches. MeHg analysis of periphyton samples collected from LEFPC EFK 5.4 in late June 2016 by Crowther et al. (2016) showed a range of MeHg concentrations of 20.1 to 33.9 ng/g dry weight of periphyton, with an average of 23.6 ng/g. Sampling conducted at EFK 13.8 on July 21, 2016, resulted in MeHg concentrations in periphyton ranging from 5.3 to 12.4 ng/g dry weight, with an average of 8.4 ng/g. These concentrations of MeHg in periphyton are consistent with the values used in the model.

Some small adjustments made to the periphyton module of the model are described in Section 3. It is recommended that as researchers obtain a better mechanistic understanding of the environmental and biological factors affecting methylation rates and periphyton concentrations, the model can be revised to incorporate these mechanisms.

➢ **HgT in periphyton calculated based on HgT on suspended solids (assumed not to be time variable)**

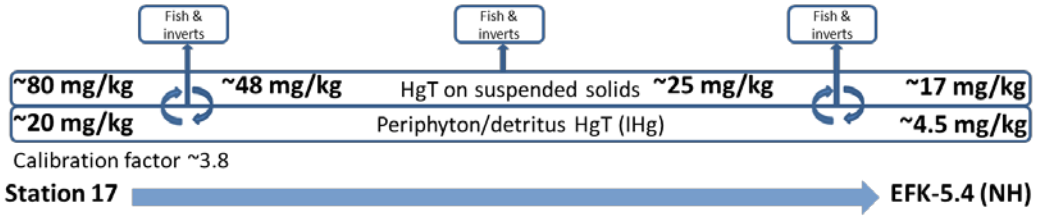

➢ **Calculation of monthly MeHg in periphyton based on MeHg in water column**

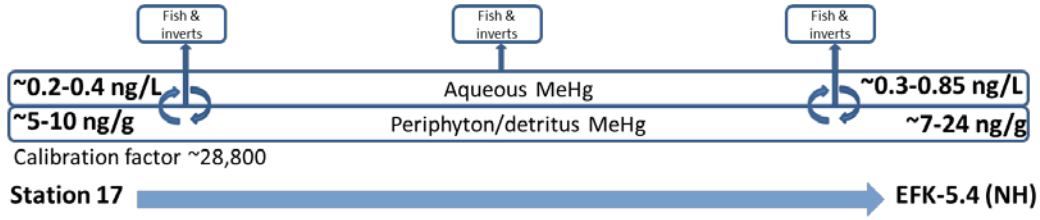

Fig. 11. Calculation of HgT and MeHg in periphyton based on HgT on suspended solids and MeHg in the lower East Fork Poplar Creek water column, respectively.

3. MODEL REVISIONS

3.1 PHYSICAL-CHEMICAL WATERSHED MODEL

Revisions to the physical-chemical watershed model included the following:

- Updated the HgT and MeHg bank erosion flux estimates for the two upstream LEFPC subwatersheds based on new characterization data available on the HRD extent and concentration
- Updated estimates of the concentration of mercury on TSS
- Changed the bank erosion calibration factor from 0.7 to 0.43 to account for the increase in the estimated bank erosion flux in the upstream LEFPC subwatersheds
- Applied the bank erosion calibration factor of 0.43 to MeHg bank fluxes (in the original model, it was not applied to MeHg fluxes)
- Increased the calibration factor for prediction of MeHg concentrations in periphyton from 25,000 to 28,800 to account for reductions in MeHg in the water column (related to reduction of MeHg bank erosion fluxes due to use of the 0.43 calibration factor)

Comparisons of the revised and original model simulations for HgT and MeHg are shown in Figs. 12 and 13, respectively. The most significant impact of these model revisions is that some of the HgT bank erosion flux was shifted to the two upstream subwatersheds, where the HRD is found, resulting in an increase in the average HgT concentration (Fig. 13) in these upstream reaches. The magnitude of MeHg flux from bank erosion decreased somewhat relative to other MeHg fluxes due to the application of the bank erosion calibration factor to MeHg (Fig. 14).

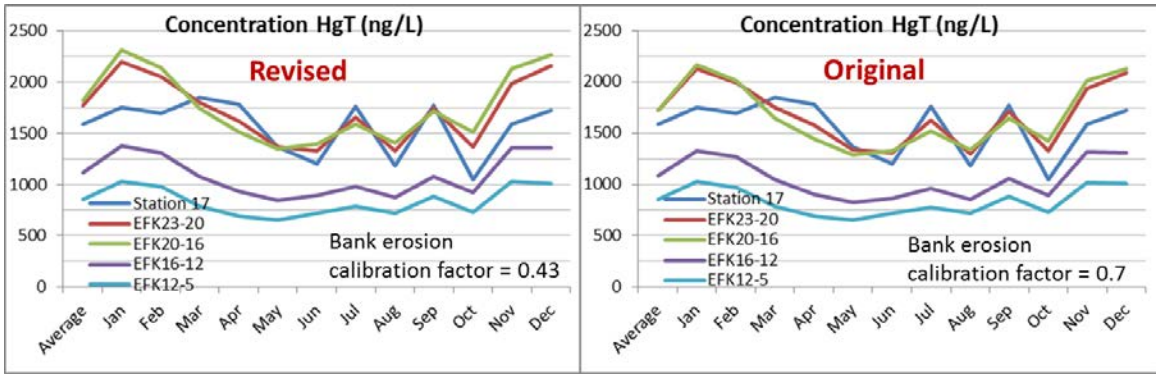

Fig. 12. Comparison of the revised and original model simulations for HgT.

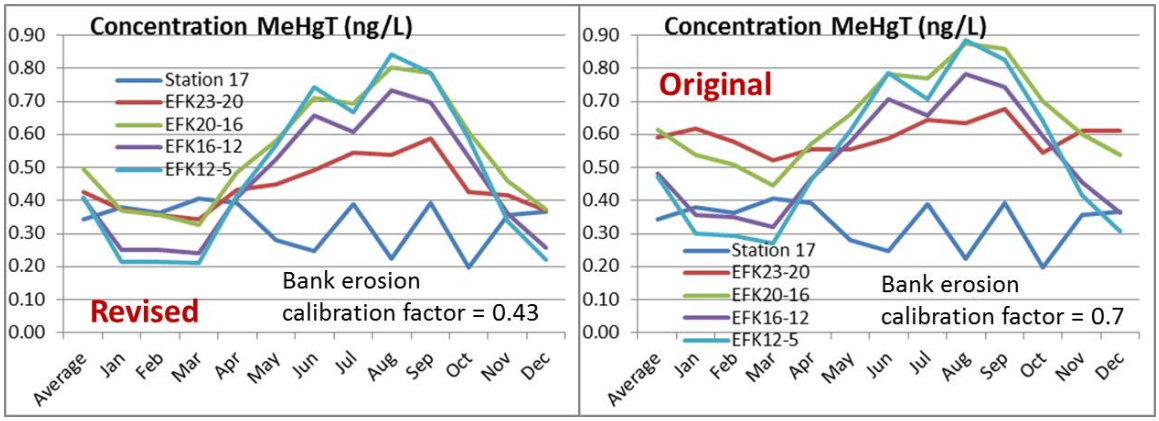

Fig. 13. Comparison of the revised and original model simulations for MeHg.

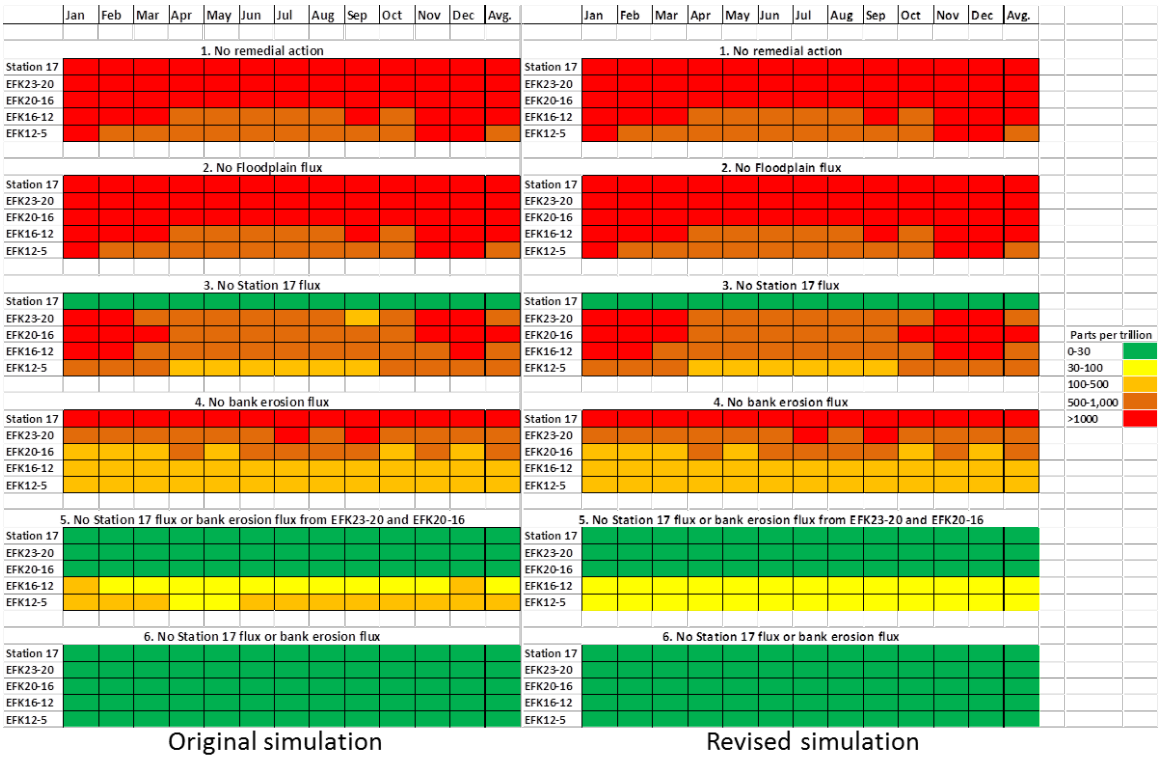

Fig. 14. Comparison of the revised and original model simulations for predicted approximate total mercury (HgT) concentrations for each source reduction scenario. (*Note:* EFK = East Fork Poplar Creek kilometer.)

Select simulations were also conducted using the revised model with input fluxes representing the various source reduction scenarios as described in Watson et al. (2016). Comparison of the revised and original model predictions of HgT concentrations for the six source reduction scenarios is shown in Fig. 14. The results for the two versions of the model are similar except for the following:

- *No Station 17 flux*—The revised simulation predicts this scenario will be somewhat less effective in the upper reaches of LEFPC, especially in the wet months when bank erosion in the upper reaches where the HRD is present is predicted to be the most active.

- *No Station 17 flux or bank erosion flux from EFK 23–20 and 20–16*—The revised simulation predicts this scenario will be somewhat more effective in the lower reaches of LEFPC, primarily because shutting off bank erosion in the upper reaches where the HRD is present is predicted to have a more significant impact on HgT flux reduction than what was predicted in the original version of the model.

3.2 BIOACCUMULATION MODELING

Model Revisions—The fish bioaccumulation model depends on inputs of periphyton MeHg concentrations from the watershed model. Incorporation of new data into the watershed model as described above resulted in new watershed model results used as new input values for the bioaccumulation model. In addition, the bioaccumulation model was improved by revising several algorithms and recalibrating the model. Revisions to the bioaccumulation model were undertaken to improve food consumption and growth dynamics, which in turn would improve predictions of MeHg accumulation in fish tissue.

The bioaccumulation model as presented in Watson et al. (2016) included different MeHg concentrations for different food types (i.e., periphyton, invertebrates, and fish) but did not include different energy contents for the different food types. Because the amount of food consumed, and therefore the amount of mercury consumed, was calculated by determining how much food intake was needed to match observed growth and energetic demands, it is important that the food intake be calculated as accurately as possible. The first iteration of the model assumed that 1 gram of food was equivalent in energy (calories or Joules) to 1 gram of consumer. However, the energy content of both periphyton and invertebrate insects is much less than fish tissue, which means that the consumption of these lower energy food items was likely underestimated in the prior model. The model now incorporates these differences in energy content (Table 3) to better predict food consumption and, therefore, MeHg consumption.

Table 3. Estimates of average energy content (Joules/g wet weight, J/g WW) of food items and consumers based on data and predictive equations from various studies

Taxa	J/g WW	Literature sources
Rock bass	6,000	Glover et al. 2010, Bowen 1987, Hartman and Brandt 1995, T. Mathews (ORNL) personal communication
Redbreast sunfish	6,000	Bevelhimer and Breck 2009, Eggleton and Schramm 2002, Miranda and Muncey 1989, Hartman and Brandt 1995, T. Mathews (ORNL) personal communication
Stoneroller minnow	5,000	Duffy 1998, Hartman and Brandt 1995, T. Mathews (ORNL) personal communication
Invertebrates	4,000	Bioenergetics 3, Wissing and Hasler 1971, Bowen 1987
Periphyton	1,500	Runck 2007, Saikia and Das 2009, Bowen 1987

Another model revision that was also related to providing more accurate estimates of food consumption was the incorporation of allometric (size-dependent) functions in the food consumption and energy efficiency equations. This change more accurately captured the decrease in relative consumption rate (i.e., grams of food/grams of consumer per day) and conversion efficiency (growth/food consumed) as fish grow larger.

Model Calibration/ Baseline Case—The above changes in the model necessitated recalibration of the model to achieve average growth rates and MeHg concentrations for each of the three modeled species as observed in reach 2, EFK 16–20. Calibration for growth was achieved by adjusting species-specific food consumption and conversion efficiency parameters. Contaminant accumulation was calibrated with

changes in the diet mixture (periphyton, invertebrates, and fish). The calibration case for reach 2 was considered the baseline for comparison against other simulation scenarios (Fig. 15).

The baseline case results clearly show the effect of age on MeHg concentrations for all three species. Precise age is nearly impossible to tell when fish are collected as part of ORNL's bioaccumulation study, and the differences seen in the model results likely explain much of the variation seen in annual samples of fish.

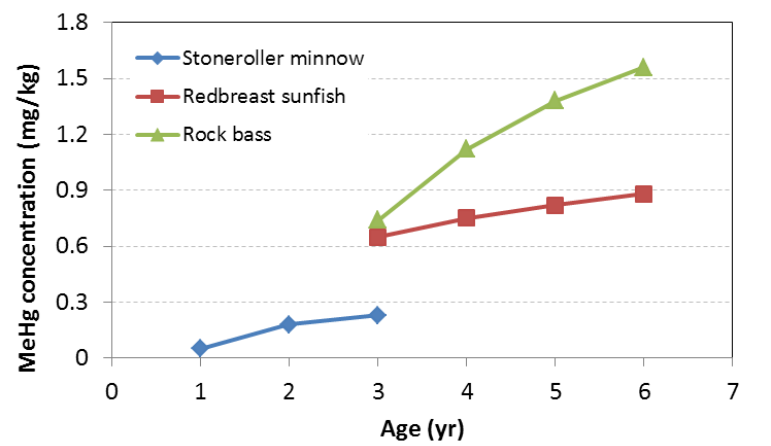

Fig. 15. Methylmercury concentrations in minnows, sunfish, and bass at ages representative of those sampled in LEFPC for body burden concentrations. (*Note:* These results represent the baseline case.)

Various simulations were run to assess other factors that contribute to variations in MeHg concentrations to better understand the system dynamics and to provide insight into possible mitigation options.

Effect of Temperature—Stream temperature affects all biological processes in one manner or another. The model includes a typical seasonal temperature variation and has a feature that allows for easily increasing the base temperature regime. In the past, flow augmentation was used as a means to reduce mercury concentrations through dilution, but a side effect of that attempted mitigation was a reduction in stream temperature. Scenarios of +/- 1 and 2°C were run to better understand the potential for affecting MeHg accumulation in the fish community. Cooler temperatures generally were found to lead to reduced MeHg concentrations in fish, assuming all other factors were constant; this was particularly true for rock bass at the top of the food chain (Fig. 16). The explanation for this is that, at warmer temperatures, energetic costs generally increase and more food must be consumed to achieve normal growth rates. Higher food consumption means that more MeHg is consumed and assimilated.

Effect of MeHg Concentrations in Periphyton—Most of the MeHg in LEFPC is believed to be generated by methylation processes in the periphyton complex (i.e., periphyton and associated detritus and bacteria). There may be mitigation measures, such as increasing shading by encouraging tree growth over the stream, that could lead to a reduction in the amount of periphyton in the stream or reduce the biological activity that produces MeHg. An evaluation was made of the effect of four levels of reduced MeHg concentrations in periphyton on rock bass, a fish at the top of the food chain. Model simulations predict that there would be a roughly one to one reduction in MeHg concentrations in rock bass (Fig. 17). That is, a 30% reduction in periphyton concentrations should result in a 30% reduction in concentrations in rock bass.

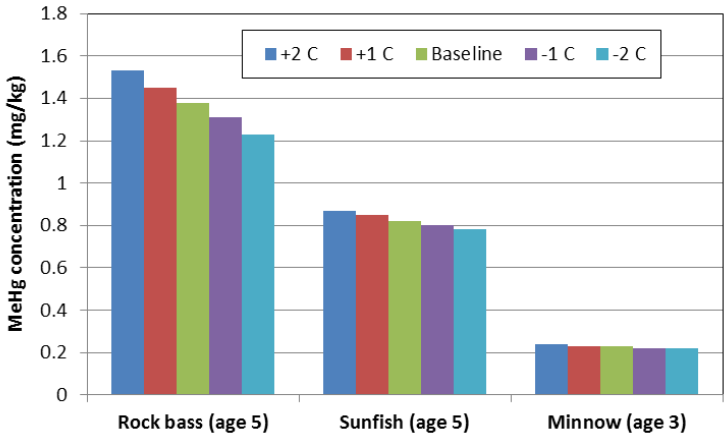

Fig. 16. Predicted MeHg concentrations in rock bass, sunfish, and minnows in response to a constant increase or decrease in stream temperature of 1 or 2°C.

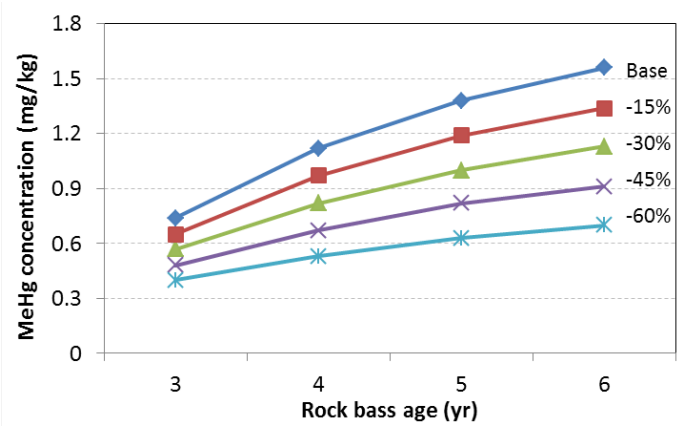

Fig. 17. Predicted MeHg concentrations in rock bass in response to decreases in MeHg concentrations in periphyton during 6-year model simulations.

Change in diet (forage base)—Biological manipulation has been used at some contaminated sites to affect trophic transfer of contaminants and reduce environmental risks. The bioaccumulation model was used to evaluate whether changes in diet composition of fish at low trophic levels could affect the MeHg concentrations in fish at the top of the food chain. In the first series of simulations, the minnow diet ratio of periphyton:invertebrates was varied from the baseline of 0.8:0.2 to a diet of increased periphyton 0.7:0.3 and to a diet of reduced periphyton 0.9:0.1. The simulated diet changes of +/- 10% in periphyton consumption by minnows is predicted to result in respective changes in rock bass MeHg concentrations of 19% (Fig. 18, left panel).

In the second series of simulations, the sunfish diet of periphyton:invertebrates was varied from the baseline of 0.1:0.9 to a diet of increased periphyton 0.2:0.8 and to a diet of reduced periphyton 0.0:1.0. The simulated diet changes of +/- 10% in invertebrate consumption by sunfish is predicted to result in respective changes in rock bass MeHg concentrations of only 3–4% (Fig. 18, right panel).

In the third series of simulations, rock bass diets were varied. The proportion of the rock bass diet that consisted of fish ranged from 50 to 90% (the rest being invertebrates), and the fish diet composed of

sunfish and invertebrates varied from 10 to 30% sunfish (the rest were minnow). These simulations revealed that the greater the proportion of fish in the diet (instead of invertebrates) and the greater the proportion of the fish diet composed of sunfish (instead of minnows), the higher the ultimate concentration of MeHg in rock bass (Fig. 19).

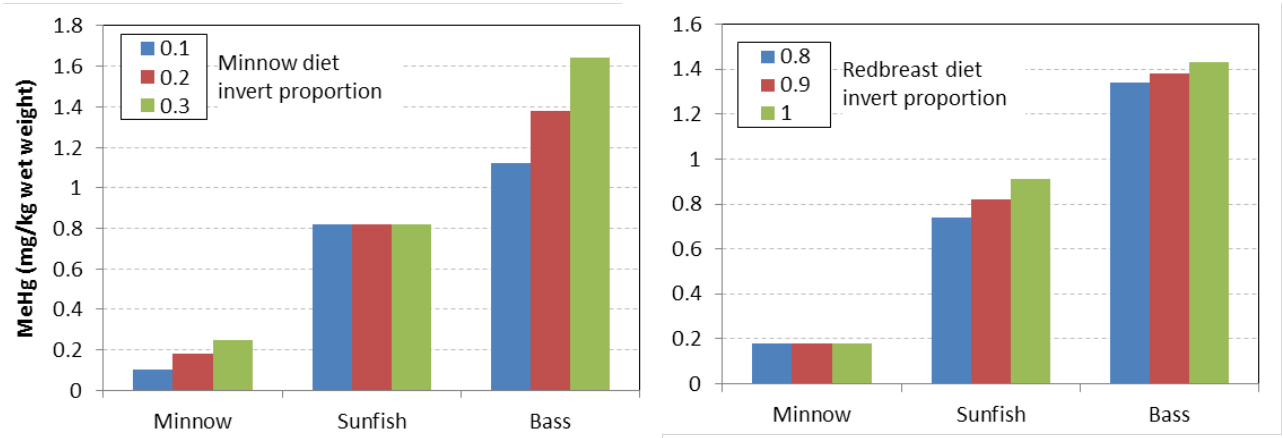

Fig. 18. Predicted MeHg concentrations in minnows, sunfish, and rock bass after (1) 10% changes (+ and -) in the proportion of minnow diet that was invertebrates (the rest were periphyton) shown in left panel and (2) 10% changes (+ and -) in the proportion of redbreast sunfish diet that was invertebrates (the rest were periphyton) shown in right panel.

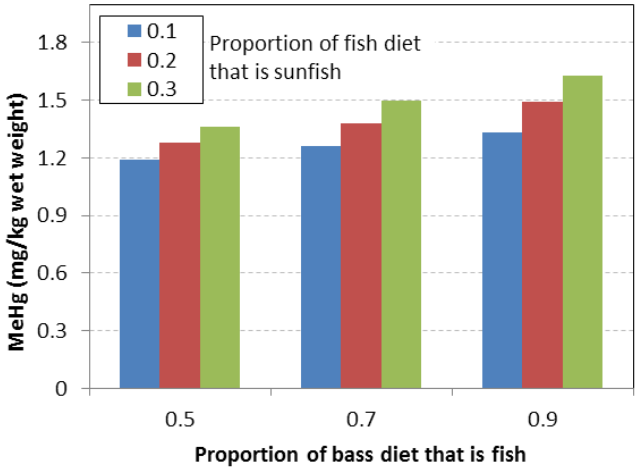

Fig. 19. Predicted MeHg concentrations in rock bass in response to changes in the proportion of the bass diet that is fish (0.5, 0.7, or 0.9; the rest is invertebrates) and the proportion of the fish diet that is sunfish (0.1, 0.2, or 0.3; the rest is minnows).

Source Reduction Scenarios—Using the revised bioaccumulation model, simulations were run again with periphyton MeHg data generated for five source reduction scenarios as described in Section 3.1. The five source reduction scenarios were compared with a baseline scenario of no remedial action. The stand-alone remedial actions of no floodplain flux and no bank erosion flux would alone produce about a 5–20% reduction in MeHg concentrations in rock bass with some variation in amount of reduction within the five stream reaches simulated (Fig. 20, upper panel). Eliminating MeHg input at Station 17 would result in a

dramatic decline in fish concentrations of MeHg in the upper creek, but elevated levels would still persist downstream. Combining the remedial action to prevent further inputs at Station 17 with cessation of bank erosion (either creek-wide or in the upper reaches only) resulted in a dramatic decline in MeHg concentrations throughout the creek in rock bass with sunfish and minnows even lower (not shown in graph). The 2016 revisions to the models and the input data produced only small changes to predicted rock bass MeHg concentrations as compared with the 2015 model runs (Fig. 20, lower panel).

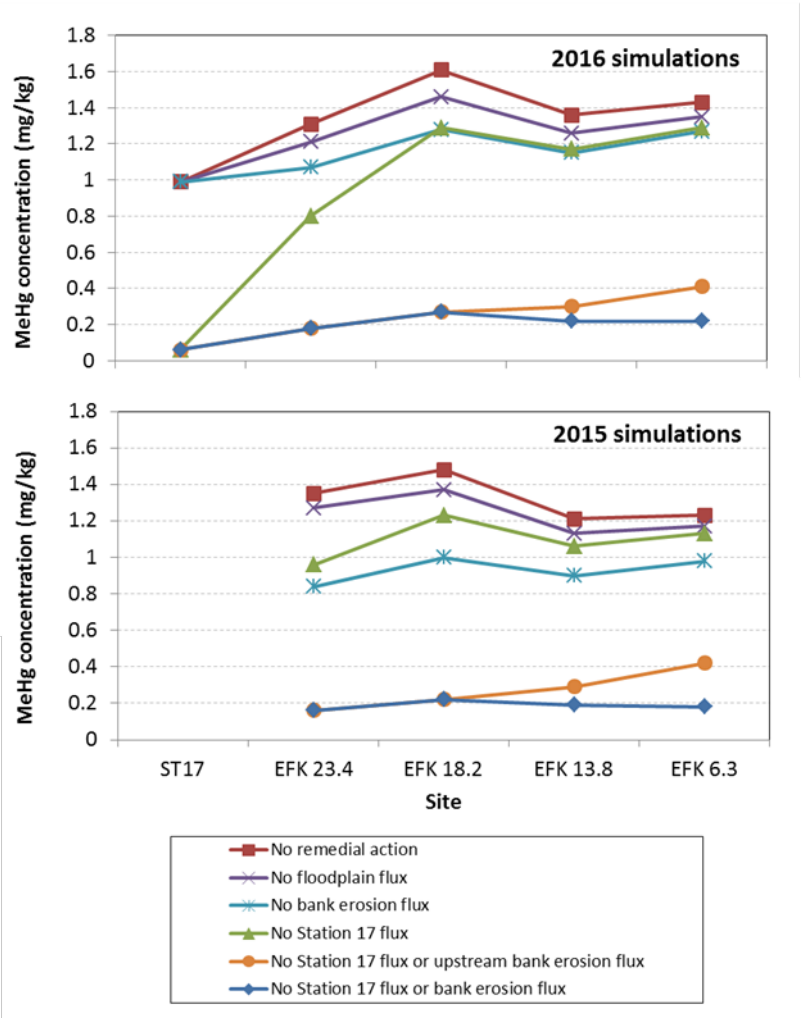

Fig. 20. Predicted MeHg concentrations in age 5 rock bass in response to five source reduction scenarios plus a no-action scenario using revised model and model inputs (2016 simulations) and original model (2015 simulations). (*Note*: Station 17 bioaccumulation was not modeled in 2015.)

4. SUMMARY AND CONCLUSIONS

Refinements to the conceptual and numerical models presented in Watson et al. (2016) were made based on new assessments of recently collected data. Where appropriate, the new data/inputs were entered into the models, and the models were rerun to determine the magnitude of changes in (1) IHg and MeHg concentrations and fluxes and (2) bioaccumulation of MeHg under baseline and various source reduction scenarios.

The key findings of the original modeling effort (Section 1) have not changed, but assessments of the new characterization data from EFPC resulted in the following insights and conclusions:

- *Station 17 flows since flow augmentation was shut off*—The average flows measured at Station 17 since flow augmentation was turned off are very close to (or slightly lower than) what was estimated and used in the model. The new flow data confirms that the original flow estimates used in the model for Station 17 are reasonable for assessing watershed fluxes but may need to be revised if UEFPC flows continue to decline.
- *Station 17 HgT flux estimates*—The average measured HgT fluxes at Station 17 (8.1 kg/yr) were slightly lower in 2015 than what is used in the model (9.8 kg/yr). However, the measured fluxes were higher than 9.8 kg/yr in the years prior to 2015. Using the lower 2015 HgT flux measurements in the model resulted in a small proportional decrease in the watershed fluxes, but this had little impact on MeHg concentrations in periphyton. Although the new flux data confirms that the original estimates used in the model for Station 17 are reasonable, they may need to be revised if UEFPC mercury fluxes continue to decline.
- *Bank erosion estimates*—New bank characterization data substantially improved the understanding of the lateral extent and concentration of the HRD and the vertical profile of HgT in the stream bank where the HRD has been observed. The bank erosion fluxes and TSS model input parameters were updated based on this new bank sampling data. To maintain mass balance, the bank erosion calibration factor had to be modified from 0.7 to 0.43. In other words, the bank erosion estimates based on the kayak data were reduced by a factor of 0.43. The revised calibration factor (i.e., 0.43) was also applied to the MeHg bank fluxes, which had the impact of reducing the estimated fluxes of MeHg from bank erosion compared with the original model.
- *Floodplain fluxes related to infiltration*—The concentrations of HgT and MeHg in new wells installed in the floodplain are on average lower but similar to the model estimates and within the bounds of what spatial and sampling variability is expected to be. The original estimated HgT and MeHg floodplain leaching fluxes were low relative to other sources of mercury fluxes in the LEFPC watershed. Incorporating this new data into the model would have made the estimates of floodplain fluxes even lower. If future investigations discover preferred pathways that are high in MeHg, this assumption should be revisited.
- *Sediment data*—The concentrations of HgT and MeHg in sediments are spatially complex but generally decrease from upstream to downstream. These trends seem to confirm that the increasing concentration trend of MeHg in LEFPC surface water is primarily related to periphyton and other biological production mechanisms and, to a lesser degree, sediment-related sources. Upstream of EFK 23, sources of sediment have fine fractions with the highest HgT concentrations of all the fractions, whereas the coarse fractions have the lowest concentrations. Downstream of EFK 23, erosion of the banks and HRD seems to provide HgT source material with higher concentrations of mercury in the medium to coarse fractions, and the concentration of mercury in the fines seems to be reduced by the influx of uncontaminated fines from the rest of the watershed. These sediment data seem to confirm

the importance of bank sources downstream of Station 17 and onsite Y-12 sources upstream of Station 17.

- *Periphyton data*—There is considerable variability in the new periphyton MeHg concentration data both spatially and over time. The variability in MeHg concentrations appears to indicate that there are complex localized environmental and biological factors controlling MeHg production in LEFPC. Despite this variability, there seems to be a general trend of higher MeHg in periphyton in middle to lower stream reaches than in upper reaches at concentrations consistent with those used in the model.

The most significant revision made to the physical-chemical watershed model was incorporating new estimates of the distribution of bank erosion fluxes and modified TSS input parameters. These revisions resulted in some of the HgT bank erosion flux being shifted to the two upstream subwatersheds where the HRD is found. The magnitude of MeHg flux from bank erosion decreased somewhat relative to other MeHg fluxes because of the application of the bank erosion calibration factor to MeHg.

Reassessment of the various source reduction scenarios with the revised model shows that removing bank erosion in the upper reaches of LEFPC where the HRD is present is more effective at reducing HgT fluxes than what was predicted with the old model (e.g., the "No Station 17 flux or bank erosion flux from EFK 23–20 and 20–16" scenario). In addition, the "no Station 17 flux" scenario will be somewhat less effective in the upper reaches of LEFPC, especially in the wet months when bank erosion in the upper reaches where the HRD is present is predicted to be the most active.

This research has produced a bioaccumulation model that demonstrates how important trophic structure and food-web dynamics are in the accumulation of MeHg in the fish community of LEFPC. Bioaccumulation and biomagnification are certainly not new concepts. However, the model enables understanding of the importance of these concepts and how the processes and rates affect MeHg dynamics through the aquatic community to the top of the food chain, where concentrations are high enough to present a human health risk. This research has demonstrated how changes in MeHg production in the periphyton matrix and changes in the diet of fish at the lowest trophic level affect MeHg concentrations in top predators. Understanding these processes allows for better evaluation of the effectiveness and magnitude of potential remedial actions.

5. FUTURE DIRECTIONS

With continued updates and refinement, the watershed-scale model will be a valuable tool for future EFPC research prioritization, technology development, and remedial decision-making. There is a continued need for field data collection and model improvements because the understanding and quantification of many mercury-related parameters and relationships is still lacking.

Recommendations for continued data collection, research and model refinement include the following:

- The HgT and MeHg fluxes at Station 17 and EFK 5.4 should be monitored simultaneously to obtain a better understanding and quantification of watershed fluxes under a variety of flow conditions.
- As new water quality monitoring data is collected and becomes available, the current assumptions used to simulate the instream HgT and MeHg processes (e.g., methylation rates) should be validated and revised as needed.
- As the watershed fluxes are reduced more substantially due to remedial actions such as the construction of the Outfall 200 (OF200) treatment plant, Y-12 facility operation modifications or continued recovery from the WEMA outfall actions the model should be updated.
- For the assessments included in this report, bedload transport of IHg and MeHg was assumed to be small relative to the fluxes of suspended and dissolved solids. Field investigations should be conducted to determine if bedload transport is an important transport mechanism of HgT and MeHg in LEFPC.
- The new sediment data coupled with the LiDAR elevation data that will become available for EFPC in FY 2017 should be used to develop a more mechanistic sediment and bedload transport module in the model. In addition, if mechanistic understanding of the causes of the spatial variability that are observed in the different size fractions of the sediment and other data is developed, then further discretization of the model into 1.0 km or smaller subwatershed segments is recommended to improve the model's predictive capabilities.
- As a better mechanistic understanding of the environmental and biological factors affecting periphyton MeHg concentrations and methylation rates is obtained, the model should be revised to incorporate these mechanisms.
- There is currently a substantial underestimation of the total estimated MeHg fluxes for EFK 5.4 related primarily to the MeHg fluxes associated with suspended solids generated during stormflow events. This should be explored to determine if the extra MeHg production may be related to undefined MeHg production (e.g., flow and methylation in undefined hyporheic zones), cyclical scouring and washing away of periphyton during storm events with regrowth of periphyton after the storm, or potential transference of the MeHg in periphyton to sediment and the water column through biological activity.

The bioaccumulation model as presented in its revised form is quite useful for understanding various processes and relationships that affect bioaccumulation of MeHg in the fish community in LEFPC and for evaluating the relative impact of potential remedial actions on bioaccumulation. However, the model also includes many parameters and relationships for which complete understanding and quantification are still lacking. Greater understanding of the following processes and mechanisms would improve the model:

- Rates of methylation by periphyton and invertebrates
- Rate of MeHg assimilation by fish from consumed food

- Demethylation or depuration of MeHg in fish
- Possible conversion of food- or water-borne inorganic mercury to tissue accumulation in fish
- More detailed diet information for LEFPC consumers

The model presently includes simply defined processes for uptake of inorganic mercury through food and water and for uptake of MeHg through water, but these pathways are currently turned off until researchers better understand the rates and relationships.

Finally, model calibration was achieved based on average concentrations from fish collected over several years from LEFPC. Because of the availability of body burden data on individual fish of known length and weight, a more sophisticated calibration can be performed based on simultaneously considering many individuals of different sizes and from different sites—instead of a calibration to an average fish that masks many of the important bioaccumulation factors. Ultimately, converting model estimates of individual fish MeHg concentrations to population-level concentrations would provide the necessary information to estimate mass flux within the fish community relative to mercury flux within the entire creek system.

6. REFERENCES

Bevelhimer, M.S., and J.E. Breck. 2009. Centrarchid Energetics, pp. 165-206. In Centrarchid Fishes: Diversity, Biology and Conservation (Editors: S.J. Cooke and D.P. Philipp). Blackwell Scientific Press.

Bowen, S.H. 1987. Composition and nutritional value of detritus, pp. 192-216. In Detritus and Microbial Ecology in Aquaculture (Editors: D.J.W. Moriarty and R.S.V. Pullin). ICLARM Conference Proceedings 14, 420 p. International Center for Living Aquatic Resources management, Manila, Philippines.

Crowther, E., T. A. Olsen, and S. C. Brooks. 2016. Diel patterns in algal metabolites. ORISE/ SULI Report. August 2016.

Duffy, W.G. 1998. Population dynamics, production, and prey consumption of fathead minnows (Pimephales promelas) in prairie wetlands: a bioenergetics approach. Can. J. Fish. Aquat. Sci. 54:15-27.

Eggleton, M.A., and H.L. Schramm, Jr. 2002. Caloric Densities of Selected Fish Prey Organisms in the Lower Mississippi River. Journal of Freshwater Ecology 17:409-414.

Glover, D.C., D.R. DeVries, R.A. Wright, and D.A. Davis. 2010. Sample Preparation Techniques for Determination of Fish Energy Density via Bomb Calorimetry: An Evaluation Using Largemouth Bass. Transactions of the American Fisheries Society 139:671-675.

Hanson, P., Johnson, T., Kitchell, J. and Schindler, D. E. 1997. Fish bioenergetics 3.0, University of Wisconsin Sea Grant Institute. Report WISCU-T-97–001, Madison, Wisconsin.

Hartman and Brandt. 1995. Estimating Energy Density of Fish. Trans. Am. Fish. Soc. 124:347-355.

Leidos. 2016 (In review). 2016 Fourth Reservation-wide CERCLA Five-Year Review for the U. S. Department of Energy Oak Ridge Reservation, Oak Ridge, Tennessee. Prepared for the U. S. Department of Energy, Office of Environmental Management. DOE/OR/01-2718&D0.

Miranda, L.E., and R.J. Muncey. 1989. Bioenergetic Values of Shads and Sunfishes as Prey for Largemouth Bass. Proc. Annu. Conf. Southeast. Assoc. Fish and Wildlife Agencies 43:153-163.

Olsen, T. A., C. C. Brandt, and S. C. Brooks. 2016 (In press). Periphyton biofilms influence net methylmercury production in an industrially contaminated system. Environ. Sci. Technol.

Peterson, M. J., et al. 2016 (In Review). Mercury Remediation Technology Development for Lower East Fork Poplar Creek - FY 2016 Progress Report. ORNL/TM-2016/494, prepared for the US Department of Energy by Oak Ridge National Laboratory, Oak Ridge, Tenn.

Runck, C. 2007. Macroinvertebrate production and food web energetics in an industrially contaminated stream. Ecol. Appl. 17(3):740-53.

Saikia, S. K., and D. N. Das. 2009. Potentiality of Periphyton-based Aquaculture Technology in Rice-fish Environment. J. Scientific Research 1 (3):624-634.

Wissing, T.E., and A.D. Hasler. 1971. Intraseasonal Change in Caloric Content of Some Freshwater Invertebrates. Ecology 52:371-373.

Watson, D.B., S. Brooks, T. Mathews, M. Bevelhimer, C. DeRolph, M. Peterson, R. Ketelle, 2016. Evaluation of Lower East Fork Poplar Creek Mercury Sources. ORNL/TM-2016/134, prepared for the US Department of Energy by Oak Ridge National Laboratory, Oak Ridge, Tenn.